ANL-7663

Argonne National Laboratory

LITHIUM/SELENIUM SECONDARY CELLS FOR COMPONENTS IN ELECTRIC VEHICULAR-PROPULSION GENERATING SYSTEMS

First Semiannual Technical Summary Report
for May 23, 1969 to November 22, 1969

by

E. J. Cairns, E. C. Gay, V. M. Kolba,
M. L. Kyle, A. D. Tevebaugh,
and L. E. Trevorrow

Printed in the United States of America
Available from
National Technical Information Service
U.S. Department of Commerce
Springfield, Virginia 22151
Price: Printed Copy $3.00; Microfiche $0.65

ANL-7663
Chemistry

ARGONNE NATIONAL LABORATORY
9700 South Cass Avenue
Argonne, Illinois 60439

LITHIUM/SELENIUM SECONDARY CELLS FOR COMPONENTS IN ELECTRIC VEHICULAR-PROPULSION GENERATING SYSTEMS

First Semiannual Technical Summary Report
for May 23, 1969 to November 22, 1969

by

E. J. Cairns, E. C. Gay, V. M. Kolba,
M. L. Kyle, A. D. Tevebaugh,
and L. E. Trevorrow

Chemical Engineering Division

Prepared for
U.S. Army Mobility Equipment Research and Development Center
Fort Belvoir, Virginia

Project Order No. MERDC 175-69
Project/Task/Work Unit IT662705A012/02/042

April 1970

FOREWORD

This is Semiannual Technical Summary Report No. 1 of a research and development program conducted by the Chemical Engineering Division of Argonne National Laboratory under an agreement with the U.S. Army Mobility Equipment Research and Development Center, Fort Belvoir, Virginia. The project order number is MERDC 175-69. The period covered by this report is May 23, 1969 through November 22, 1969.

The long-term goal of this program is to develop the technology for construction and testing of 50-kW lithium/selenium secondary batteries for use in military vehicles. The immediate goals are the scale-up and testing of single lithium/selenium cells (31.6-cm^2 active area), followed by the construction and testing of small (near 1 kW) batteries.

Overall program management is the responsibility of Dr. R. C. Vogel, Division Director, and Dr. A. D. Tevebaugh, Associate Division Director. Technical direction is provided by Dr. E. J. Cairns, Section Head, and Dr. E. C. Gay, Problem Leader. The Contracting Officer's Technical Representative is Dr. J. R. Huff.

TABLE OF CONTENTS

ABSTRACT 1

I. INTRODUCTION 1

II. LITHIUM/SELENIUM CELL STUDIES 2
A. *LITHIUM/SELENIUM CELL ELECTRICAL-PERFORMANCE STUDIES* 2
B. *LIFE TESTING AND CHARGE-DISCHARGE CYCLE TESTING OF LITHIUM/SELENIUM CELLS* 9
C. *DESIGN OF HIGH-SPECIFIC-POWER LITHIUM/SELENIUM CELLS* 10

III. PASTE-ELECTROLYTE STUDIES 10
A. *PHYSICOCHEMICAL PROPERTIES OF PASTE ELECTROLYTES* 10
B. *FABRICATION OF 7.5-cm-diam PASTE-ELECTROLYTE DISKS* 13

IV. SEALANTS AND INSULATORS 15

V. CORROSION BY LITHIUM-SELENIUM MIXTURES 16

VI. CONCLUSIONS 18

VII. FUTURE WORK 18

REFERENCES 19

LIST OF FIGURES

1. Components of 7.5-cm-diam Paste-electrolyte Cells 2
2. Lithium/Selenium Cell Components 3
3. Voltage-Capacity Density Curves for Lithium/Selenium Cells No. 6 and 7 4
4. Voltage-Capacity Density Curves for Lithium/Selenium Cells No. 2, 5, and 8 5
5. Voltage-Current Density Characteristics for Lithium/Selenium Cells No. 5, 7, and 8 6
6. Voltage-Capacity Density Curves for Lithium/Selenium Cell No. 1 6
7. Voltage-Current Density Characteristics for Lithium/Selenium Cell No. 2 7
8. Voltage-Current Density Characteristics for Lithium/Selenium Cell No. 3 7
9. Proposed 7.5-cm-diam Paste-electrolyte Test Cell 10
10. Circuit Diagram of Apparatus for Electrolyte Resistance Measurements by a DC Method 11
11. Sample-holder Assembly No. 2 for Resistance Measurements in Paste-electrolyte Disks 12
12. Corrosion by Lithium-Selenium Mixtures 17

LIST OF TABLES

I. Characteristics of Lithium/Selenium Cells Using 7.5-cm-diam Paste Electrolytes 4
II. Electrical Performance of 31.6-cm^2 Lithium/Selenium Cells at 400°C 5
III. Values for Variables To Be Used in Cell Life Tests 9
IV. Properties of Paste-electrolyte Disks 11
V. Densities of 7.5-cm-diam Paste Electrolyte Prepared under Various Conditions at 56,600-kg Force Using LiF-LiCl-LiI Eutectic Electrolyte 14
VI. Thermal Stability of Polymeric Materials in a Helium Atmosphere 15
VII. Corrosion Resistance of Polymeric Materials to the Lithium-Selenium System 16
VIII. Outline of Battery Materials Requirements 16
IX. Corrosion by 20 at. % Lithium-Selenium Mixtures 17
X. Approximate Composition of Alloys Tested in Lithium-Selenium Mixtures 17

LITHIUM/SELENIUM SECONDARY CELLS FOR COMPONENTS IN ELECTRIC VEHICULAR-PROPULSION GENERATING SYSTEMS

First Semiannual Technical Summary Report
for May 23, 1969 to November 22, 1969

by

E. J. Cairns, E. C. Gay, V. M. Kolba,
M. L. Kyle, A. D. Tevebaugh,
and L. E. Trevorrow

ABSTRACT

Eight lithium/selenium cells with 7.5-cm-diam paste electrolyte (44.2-cm^2 total area, 31.6-cm^2 active area) have been designed, fabricated, and tested. Short-time peak-power densities up to 2 W/cm^2 were delivered by these cells, and up to 60% of the theoretical capacity density was achieved (at 0.15 A/cm^2). Cell lives of 50 hr (10 cycles) have been demonstrated. Lack of wetting of paste electrolyte by lithium in some cells has resulted in high internal resistance and correspondingly poor electrical performance. Vapor deposition of lithium on the paste before assembly of the cell may alleviate this wetting problem.

Initial measurements of paste-electrolyte resistivities indicate that resistivity ratios as low as 3 may be achievable. Materials stability and corrosion tests have shown that a few high-temperature polymers are stable at 375°C, but are not resistant to lithium at that temperature. Several ceramic materials, which could serve either as fillers or electronic insulators, are resistant to lithium at 375°C. The metals most resistant to lithium-selenium mixtures at this temperature are beryllium, niobium, Nb-1% Zr, and chromium.

I. INTRODUCTION

The secondary lithium/selenium batteries being developed at Argonne National Laboratory have projected capabilities appropriate for use in hybrid (turbine-battery) electrically driven military vehicles. The ANL batteries, which will operate in the range of 400°C and below, will be composed of cells with liquid-lithium anodes, immobilized fused-salt electrolytes (in the form of rigid paste), and liquid-selenium cathodes. Typical short-time peak-power densities for lithium/selenium cells of 3.8-cm^2 active area are 1-3 W/cm^2. Results for these cells suggest that properly designed multikilowatt batteries should store 360 W-hr/kg (6-hr rate) and deliver power at 130 W/kg (1-hr rate) [1].

The electrode reactions in the lithium/selenium cell during discharge are as follows:

$$\text{Anode } xLi \rightarrow xLi^+ + xe^-; \quad (1)$$

$$\text{Cathode } xLi^+ + ySe + xe^- \rightarrow Li_xSe_y. \quad (2)$$

The largest lithium-to-selenium atom ratio achieved in the cathode during cell discharge corresponds to the stable compound Li_2Se. This stoichiometry is the basis for calculation of the theoretical capacity densities reported below. Reactions 1 and 2 are carried out in the reverse directions during recharge of the cell.

Reactions 1 and 2 are reversible and can take place at very high rates with very little loss in cell voltage. The exchange-current densities are in the range of several amperes per square centimeter. Because of this, the only voltage losses in a lithium/selenium cell are those due to the internal resistance of the cell (resistance overvoltage) and slow mass transport in the selenium electrode (diffusion overvoltage).

The effort for development of these cells is concentrated in the following areas:

Task A. Lithium/selenium cell studies for electric vehicle propulsion

1. Lithium/selenium cell electrical-performance studies
2. Life-testing and charge-discharge cycle testing of lithium/selenium cells
3. Design of high-specific-power lithium/selenium cells
4. Automatic charge-discharge testing of multiple lithium/selenium cells

Task B. Studies of paste electrolytes for lithium/selenium cells

Task C. Studies of sealants and insulators for lithium/

selenium cells

Task D. Studies of corrosion by lithium-selenium mixtures

Task E. Lithium/selenium battery studies

The objective of Task A (involving cell studies) is the development of 7.5-cm-diam cells (31.6-cm^2 active area) having 1-3 W/cm^2 short-time peak-power density and having a long life (1000-2000 hr and 1000-2000 cycles). To achieve this objective, the current density-voltage and voltage-time behaviors of the cells are determined and cell design changes are made as required to improve the electrical performance. The porosity, pore-size distribution, and structural configuration of the cathode-current collector are being optimized so that the maximum power density is obtained for the largest fraction of theoretical cell capacity.

Task B provides information on techniques required to fabricate large-area paste electrolyte of high strength and low electrolytic resistivity. This area of investigation will assume particular significance as methods are required to fabricate paste-electrolyte disks of larger diameter (up to 18 cm). The objective of Task B is the optimization of the physical and electrochemical properties of the paste electrolyte, which should have maximum strength and minimum electrolytic resistivity in order to serve as a reliable, minimum-weight, low-resistance separator between anode (lithium) and cathode (selenium). The strength of the paste electrolyte is maximized by use of a high-specific-area ceramic filler material; the resistivity is decreased by increasing the fuzed-salt content. Paste-electrolyte optimization involves the preparation of paste electrolyte with the maximum fused-salt content consistent with good strength.

The objective of materials study Tasks C and D is to identify corrosion-resistant metals, alloys, and insulators that are lightest in weight, easy to fabricate, least expensive, and consistent with long operating life.

The objective of Task E (battery design, construction, and testing) is the development of reliable batteries, probably starting with 1-kW laboratory test batteries and eventually progressing to 50-kW prototypes.

This report summarizes the progress on the above tasks from May 23 to November 22, 1969.

II. LITHIUM/SELENIUM CELL STUDIES

Several lithium/selenium cells with 7.5-cm-diam paste electrolytes have been constructed and tested. The details of the cell design and assembly are given below, followed by the test results for the individual cells.

A. LITHIUM/SELENIUM CELL ELECTRICAL-PERFORMANCE STUDIES (E. C. Gay and J. E. Kincinas)

The electrical performance of the cells is evaluated in terms of voltage-current density and voltage-time behavior (capacity measurement) during constant-current discharge as a function of cell structure and number of charge-discharge cycles. The porosity, pore-size distribution, and structural configuration of the cathode-current collector will be varied to determine the best design for high power density and high fraction of theoretical capacity density.

Experiments were conducted with the objective of developing scaled-up lithium/selenium cells having the same short-time power-density capabilities as the 2.5-cm-diam paste-electrolyte cells (1-3 W/cm^2). No attempt was made during these initial tests to determine cell life or maximum number of charge-discharge cycles. During the reporting period (May 23 to November 22), the electrical performance of eight cells with 7.5-cm-diam paste electrolytes was determined.

1. Cell Components

Figure 1 shows a schematic diagram and cross-sectional views of two assembled 7.5-cm-diam paste-electrolyte cells used for electrical-performance measurements; Fig. 2 shows typical cell components. All the cells were operated with the paste electrolyte in the vertical position, with about 50% voids in the cathode compartment to allow for lithium

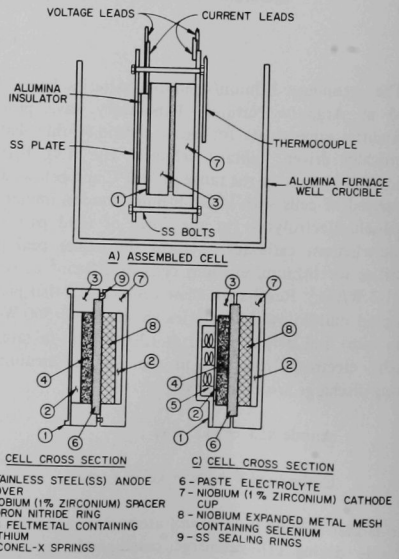

Fig. 1. Components of 7.5-cm-diam Paste-electrolyte Cells.

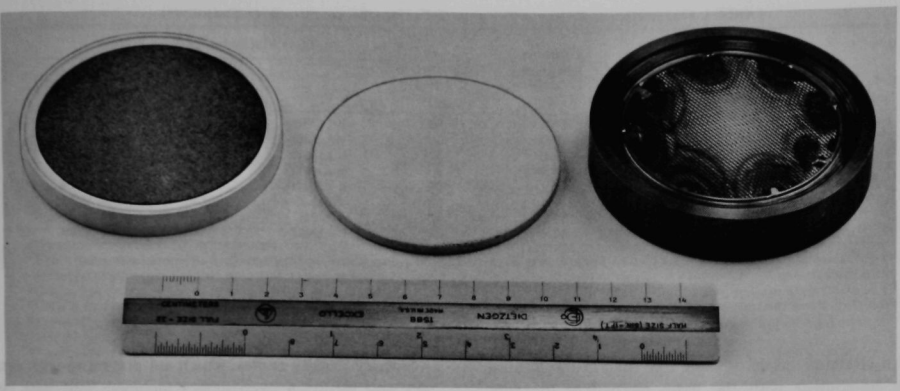

Fig. 2. Lithium/Selenium Cell Components (left to right): (a) Boron Nitride Anode Ring and SS Feltmetal Current Collector; (b) 7.5-cm-diam Paste Electrolyte; (c) Niobium Cathode Compartment and Niobium Expanded Mesh Current Collector.

transfer. With tightly stacked mesh in the cathode compartment, the voids were distributed randomly throughout the compartment. With loosely stacked mesh, the voids occupied the upper portion of the compartment as selenium collected in the lower portion upon heating the cell. In the early tests (Cells No. 1 to 5), a boron nitride ring insulated the anode from the cathode compartment and also served as part of the anode housing. In some cases, stainless steel sealing rings (0.16 and 0.08 cm thick) or stainless steel O rings (0.16-cm-diam tubing) were used with the cell housings (stainless steel anode cover, boron nitride ring, and niobium cathode cup) as shown in Fig. 1B. The thickness of the sealing rings was such that both the paste electrolyte and the stainless steel rings seated against the boron nitride and the niobium cathode cup. (The effectiveness of the seal was established by the fact that the cell lost no weight during operation.) Cathode voltage and current leads were attached to the cell clamp, and the clamp was insulated from the anode by an alumina disk. The anode voltage and current leads were welded to the stainless steel anode cover. Modifications (shown in Fig. 1C), which were made in this assembled cell configuration for some of the tests, will be discussed where applicable in the description of the electrical performance of the eight cells.

The anode and cathode compartments of the cell are shown in Fig. 2. The anode consisted of stainless steel Feltmetal (Huyck Metal Co.: Type 302 stainless steel, 1.6 mm thick, 90% porosity, 67-μ mean pore size; or Type 430 stainless steel, 6.4 mm thick, 87% porosity, 50-μ mean pore size) that had been soaked with lithium at 550°C. The cathode consisted of niobium expanded mesh of approximately 63% porosity (0.23-cm die size). Sheets of the niobium mesh were welded together and welded to the inner surface of the niobium cathode cup. The paste electrolyte and the quantities of lithium and selenium loaded into the various cells are described in Table I.

The paste electrolytes used in cells tested were prepared using lithium aluminate filler (of approximately 46-m^2/g surface area) and LiF-LiCl-LiI eutectic. This eutectic has a composition of 11.7 mol % LiF-29.1 mol % LiCl-59.2 mol % LiI and a melting point of 340.9°C. The resistivity at 400°C (the operating temperature for most of the cells in this report) is 0.405 ohm-cm (from Ref. 2). The fillers used in the paste electrolyte were α-$LiAlO_2$, γ-$LiAlO_2$, or a mixture of these materials. These fillers are prepared by the reaction of γ-Al_2O_3 with Li_2CO_3. The α-$LiAlO_2$ is the major product at reaction temperatures around 600°C; the γ-$LiAlO_2$ is the major product at 800°C. Attempts to prepare large batches of the filler for use in the cells described above resulted in a mixture of α- and γ-$LiAlO_2$. No differences in electrical performance have been observed using paste electrolyte prepared from either. Pressing conditions for paste electrolytes are given in Section III.A.1.

Cell-component design and paste-electrolyte preparation procedures were changed during the testing of the initial eight cells to improve the cell performance. The following features appear to be necessary for good electrical performance:

a. The stainless steel Feltmetal containing lithium should be spring-loaded to provide good electrical contact with the paste electrolyte.

b. The paste-electrolyte molding powder should not contain sources of oxygen, such as moisture, unreacted Al_2O_3, or carbonate and should be readily wet by lithium and selenium. Also, for high strength, the paste electrolyte should have a density in excess of 90% of the theoretical value.

TABLE I. Characteristics of Lithium/Selenium Cells Using 7.5-cm-diam Paste Electrolytes

Cell No.	Theoretical Capacity,[a] A-hr	Anode Lithium Content, g	Cathode Selenium Content, g	Paste Electrolyte			
				Electrolyte Content,[b] wt %	Filler	Fraction of Theoretical Density	Thickness, cm
1	9.8	4.1	14.4	50	α-$LiAlO_2$	0.89	0.22
2[c]	20.2	4.3	29.7	60	α-$LiAlO_2$	0.77	0.26
3	16.7	5.2	24.6	60	α-$LiAlO_2$	0.70	0.28
4	19.6	8.3	28.9	60	γ-$LiAlO_2$	0.77	0.30
5	20.5	9.9	30.1	60	α-$LiAlO_2$	0.85	0.24
6	16.4	9.1	24.1	60	α-$LiAlO_2$	0.92	0.23
7	19.4	7.1	28.5	60	α-$LiAlO_2$	0.83	0.26
8	18.5	9.5	27.2	60	α-$LiAlO_2$	0.91	0.26

[a]This theoretical capacity was based upon Li_2Se as the fully discharged composition and the quantity of selenium loaded into the cathode.
[b]The electrolyte used in preparing the paste disks was the LiF-LiCl-LiI eutectic; m.p. = 340.9°C.
[c]Cell No. 2 was the only anode-limited cell tested.

c. An electrical insulator should be used at the lithium housing in contact with the paste electrolyte to avoid deposition of lithium outside the cell during charging.

d. The cathode-current collector should be welded to the cathode housing to reduce cell internal resistance.

No attempt was made to minimize the cell weight in these first experiments. The major objective was to design cells that would provide a power density of about 2 W/cm^2. The design of high-specific-power cells is discussed in Section II.C. below.

2. *Experimental Procedures for Electrical-performance Testing*

The components of the 7.5-cm-diam paste-electrolyte cells were assembled as described above. The assembled cell was mounted in a furnace that was attached to the floor of a helium-atmosphere glovebox and heated by an electric-resistance furnace.

The cells were charged and discharged at constant currents with the aid of a high-current dc power supply. Usually, discharge data were taken at the fully charged condition (open-circuit voltage of 2.2 V), and charge data were taken at the partially discharged condition. The cell resistance was determined from short-time data (a few seconds after closing the circuit) of cell voltage as a function of current density. These measurements were made so rapidly that there was a negligible overvoltage due to mass-transport of reactants to, or removal of, products from the paste-electrolyte/cathode interface (<0.02 V).

The resistance overvoltage is the sum of (1) the overvoltages caused by the electronic resistance of the accumulated cell reaction products at the cathode/electrolyte interface, (2) the contact resistance associated with insufficient wetting of the paste electrolyte by the electrode materials, (3) the electrolytic resistance of the paste electrolyte, and (4) the resistance of corrosion products formed on some current-collector materials. The cell voltage was measured as a function of time during constant-current discharge. These curves were used to calculate the voltage-*vs*-capacity density curves, which are presented with resistance and diffusion overvoltages included, and with only diffusion overvoltage included. The voltage difference between these curves is the resistance overvoltage. These curves are termed "IR-included" and "IR-free," respectively. The theoretical capacity was calculated assuming the fully discharged cathode composition to be Li_2Se. All current-density and capacity-density values were based on the active paste-electrolyte area of 31.6 cm^2.

3. *Electrical Performance*

The electrical performance of the cells is summarized in Table II. The maximum capacity obtained for a 7.5-cm-diam paste-electrolyte cell was 11.4 A-hr (0.36 A-hr/cm^2); this value, which corresponds to 58.8% of the theoretical capacity, was achieved with Cell No. 7. The voltage-capacity curve (shown in Fig. 3) was measured at 400°C and 0.15 A/cm^2 (4.8 A). The average cell voltage during discharge of Cell No. 7 was 1.6 V. The maximum short-circuit current density obtained for a 7.5-cm-diam paste-electrolyte cell

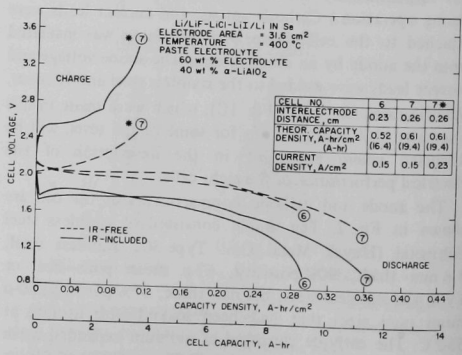

Fig. 3. Voltage-Capacity Density Curves for Lithium/Selenium Cells No. 6 and 7.

TABLE II. Electrical Performance[a] of 31.6-cm^2 Lithium/Selenium Cells at 400°C[b]

Cell No.	Peak Power Density W/cm^2	Discharge Current Density, A/cm^2	Average Discharge Voltage,[c] V	Discharge Time, hr	Capacity Density, A-hr/cm^2	Energy Density, W-hr/cm^2	Fraction of Theoretical Capacity	Resistivity Ratio[d]	Fraction of 1-hr Current Density[e]
1	0.3	0.02	1.0	1.0	0.02	0.02	0.20[f]	40	0.067
2	0.7	0.05	1.3	6.4	0.32	0.42	0.61	15	0.17
3	0.4	-	g	-	-	-	-	45	-
5	2.0	-	g	-	-	-	-	6	-
6	0.6	0.15	1.6	1.9	0.29	0.46	0.55	18	0.50
7	0.6	0.15	1.6	2.4	0.36	0.58	0.59	18	0.50
8	1.0	0.52	1.4	0.4	0.22	0.31	0.38	11	1.7

[a]No attempts were made to test cells for long periods of time or large numbers of charge-discharge cycles. Cell 1 was tested for 120 hr and 25 charge-discharge cycles (longest period tested and highest number of cycles). Other cells were tested for about 48 hr (10 cycles maximum) at the discharge rates indicated.
[b]Cell 3 was tested at up to 600°C.
[c]Cells 5 through 8 were discharged to 1.0 V. Cell 2 was discharged to 0.5 V, and Cell 1 was discharged to 0.1 V.
[d]Ratio of paste electrolyte resistivity to LiF-LiCl-LiI eutectic resistivity. These values are the lowest ratios observed over the test period.
[e]This current-density ratio is the discharge current density divided by the current density (0.3 A/cm^2) for a 1-hr discharge time to 1 V.
[f]Selenium escaped from this cell resulting in a low fraction of theoretical capacity measured.
[g]No capacity measurements were made for these cells.

(No. 5) was 3.8 A/cm^2 (120 A). This cell was discharged at 0.31 and 0.49 A/cm^2 (9.7 and 15.6 A). The average cell voltages during these discharges were 1.75 and 1.54 V, respectively. These results are shown in Figs. 4 and 5. The lowest measured resistivity ratio (the ratio of paste-electrolyte resistivity to LiF-LiCl-LiI eutectic resistivity) was 6 for Cell No. 5. High resistivity values result from poor wetting of the paste electrolyte by lithium at the anode-electrolyte interface. The lower limit for the resistivity ratio is being determined from investigations carried out in the paste-electrolyte studies task; any required changes will be made in the cell design or assembly to achieve this lower limit.

The sections below discuss the assembly and testing of the eight cells.

a. Test Results for Cell No. 1

This first experiment was intended to identify the major problem areas requiring solution in order to develop scaled-up cells having the same power-density capabilities as 2.5-cm-diam paste-electrolyte cells. This was the first 7.5-cm-diam paste-electrolyte cell tested and thus the first attempt to seal a scaled-up cell and obtain electrical-performance data.

Typical voltage-capacity curves for Cell No. 1 under constant-current discharge are presented in Fig. 6. The cell was operated for 120 hr and 25 charge-discharge cycles. The discharge rates for this cell are shown in Fig. 6. The maximum capacity obtained was 0.89 A-hr on the fourth day of testing, which corresponds to about 20% of the theoretical capacity (4.48 A-hr). During testing, selenium escaped from the cell, causing a loss of capacity.

A comparison of the resistance overvoltages in discharges 1 and 19 (as shown in Fig. 6) indicated that these losses were much smaller in discharge 19. (The low cell voltage for discharge 19 is typical of cells in which the selenium has escaped due to poor sealing.) A large portion of the resistance overvoltage was a result of poor wetting of the paste-electrolyte. The effect of paste-electrolyte wetting (lithium side) on the voltage-capacity curve is shown in discharge 1. As the paste electrolyte begins to wet, the lithium transfer area increases (lowering the resistance overvoltage), and the cell voltage increases at constant current. This increase of voltage with time of operation (increased wetting of the paste electrolyte) and with temperature was previously observed in performance tests of smaller (2.5-cm-diam) cells. The time required for paste-electrolyte wetting varies with the properties of the paste electrolyte and may be as short as 5 min.

The maximum short-circuit current density obtained during short-time voltage-current measurements was 0.54 A/cm^2. The resistivity ratio of the paste electrolyte to the

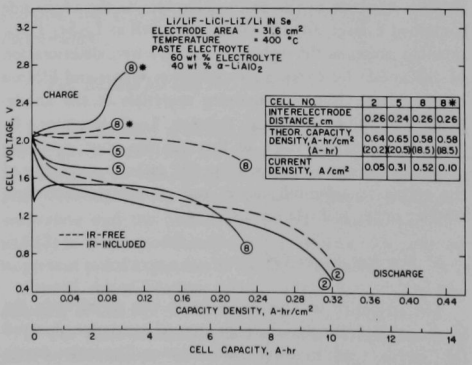

Fig. 4. Voltage-Capacity Density Curves for Lithium/Selenium Cells No. 2, 5, and 8.

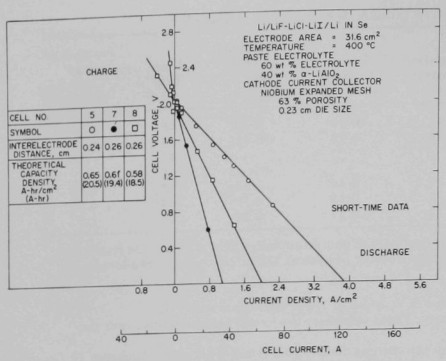

Fig. 5. Voltage-Current Density Characteristics for Lithium/Selenium Cells No. 5, 7, and 8.

pure electrolyte was 151, 55.6, and 40, respectively, for the first (and second), third, and fourth days of testing. These values can be compared with a theoretical resistivity ratio of 2.2 for this paste electrolyte with an electrolyte volume fraction of 0.552 (50 wt % filler).

As determined from the slope of the voltage-current density curves for the first and second days of testing, the amount of wetting had not been sufficient to decrease the resistance overvoltage to the expected value. Beyond the second day of testing, however, the resistance overvoltage decreased with time. A comparison of the resistance for the third and fourth days showed that the latter was 21% lower. However, the open-circuit voltage had decreased on the fourth day (typical of conditions in the smaller cells when small cracks formed in the paste electrolyte), thus reducing the short-circuit current density.

Analyses of samples from this first cell indicated that the product adjacent to the paste electrolyte on the anode side contained a large amount of Li_2O as well as Li_2Se. Thus, possible causes of the high cell resistance were deterioration of the anode by exposure to selenium vapors and lithium reaction with oxygen-containing materials at the anode-paste electrolyte interface forming Li_2O insulator. In general, the performance of this cell was poor, probably because of selenium escape from the cathode, exposure of the anode to selenium vapor, and poor paste-electrolyte wetting owing to Li_2O formation.

b. Test Results for Cell No. 2

The objective of this experiment was to identify the factors contributing to the high internal resistance observed for Cell No. 1 and to lower this resistance. The major design change consisted of welding the cathode-current collector to the cathode housing. Also, steps were taken to reduce exposure of the paste electrolyte to atmospheric moisture and to reduce the carbonate and aluminum oxide content in the filler used to prepare the paste electrolyte. (Sources of oxide in the electrolyte were believed to contribute to the cell resistance by the formation of Li_2O.)

The voltage-capacity curve at the start of operation is presented in Fig. 4. The cell was operated for 96 hr (10 cycles) and was discharged to 0.5 V. The maximum capacity obtained was 10.1 A-hr (0.32 A-hr/cm^2). This value corresponds to 50% of the theoretical capacity. (The cell was assembled with 7.6% excess selenium.) The 10.1-A-hr capacity was measured during the initial discharge at 405°C (1.5 A for 6.75 hr at an average cell voltage of 1.3 V).

During short-time voltage-current measurements taken at the start of cell testing, a short-circuit current density of 1.3 A/cm^2 (41 A) was obtained, as shown in Fig. 7. The resistivity ratio (ratio of paste-electrolyte specific resistance to the pure-electrolyte specific resistance) was 15.4, compared with a theoretical value of 1.8. The paste-electrolyte resistivity ratio for Cell No. 2 was considerably lower than that for Cell No. 1.

To some extent, the higher current densities achieved with the second cell as opposed to the first (1.3 *vs* 0.54 A/cm^2 on short circuit) may be attributed to the welding of the cathode-current collectors to the cathode cup.

After Cell No. 2 had been left on open circuit at 405°C over the first night, its electrical performance decreased considerably. A slight increase of electrical performance was obtained by increasing the cell temperature to 534°C and maintaining the higher temperature during further testing. Decreasing the cell temperature resulted in a decrease of the electrical performance. The cause of the loss of cell performance and the mechanism for the performance gain caused by raising the temperature have not been determined at this time.

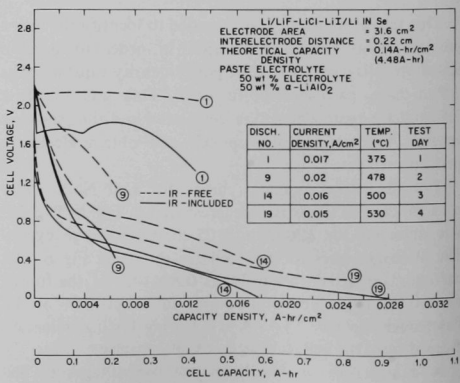

Fig. 6. Voltage-Capacity Density Curves for Lithium/Selenium Cell No. 1.

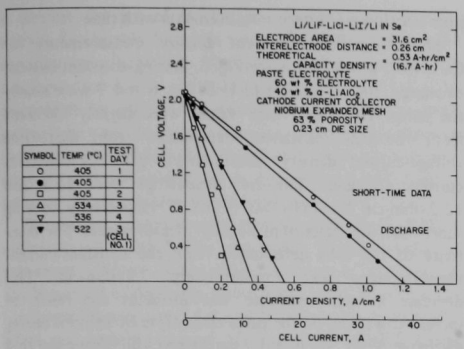

Fig. 7. Voltage-Current Density Characteristics for Lithium/Selenium Cell No. 2.

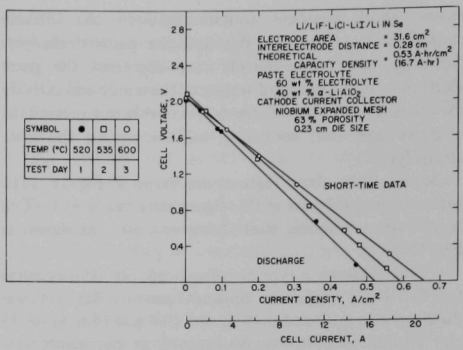

Fig. 8. Voltage-Current Density Characteristics for Lithium/Selenium Cell No. 3.

The short-time voltage-current density measurements showed that the resistivity ratio increased from 15.4 on the first day of testing to approximately 55.6 on the fourth day of testing. The latter resistivity ratio was nearly the same as that observed before shutdown of Cell No. 1.

An examination of the anode-current collector at shutdown indicated that the stainless steel felt had reacted with selenium. A crack in the paste electrolyte at the cathode sealing surface had exposed the lithium-soaked stainless steel anode-current collector to selenium vapors. Higher-strength paste electrolytes are needed to avoid this problem.

c. Test Results for Cell No. 3

The objective of this experiment was to determine the effect of temperature on the wetting of the paste electrolyte by lithium. In previous experiments, increased wetting of the paste electrolyte was observed with increased operating temperature. Poor wetting of the paste electrolyte (mainly a problem on the lithium side of the paste electrolyte) contributes substantially to the internal resistance of the cell.

The short-time voltage-current density results for Cell No. 3 are shown in Fig. 8. Although the internal resistance of the cell decreased slightly after three days of testing at temperatures between 520 and 600°C, the resistance was much higher than that measured for Cell No. 2 during the period of its best performance. The best short-circuit current density measured for Cell No. 3 was 0.66 A/cm² (21.7 A), compared with 1.3 A/cm² (41 A) for Cell No. 2. Temperatures between 520 and 600°C were used during this test because it was believed that poor paste-electrolyte wetting might be caused by Li_2O formation from such sources as adsorbed moisture on the paste-electrolyte surface. High temperatures would increase the solubility of Li_2O in lithium to enhance the removal of Li_2O from the paste-electrolyte surface and result in better wetting.

The following conclusions were drawn from the large difference in resistivity (6.2 and 14.0 ohm-cm for Cells No. 2 and 3, respectively): (1) Although paste-electrolyte wetting is an important factor in cell performance, this factor alone does not appear to account for the resistivity differences observed between Cells No. 2 and 3. (2) Wetting is enhanced by operating the cell at high temperatures, but not sufficiently to warrant the use of high temperatures.

d. Test Results for Cell No. 4

The objective of this experiment was to determine the effect of a paste electrolyte containing γ-$LiAlO_2$ filler (low carbonate and Al_2O_3 content, *i.e.*, low sources of oxygen) instead of α-$LiAlO_2$ on cell performance. The paste electrolyte cracked during the first day of testing. The testing period for Cell No. 4 was therefore too short to compare the effects of γ-$LiAlO_2$ and α-$LiAlO_2$ on cell performance.

e. Test Results for Cell No. 5

The objectives of this experiment were (1) to determine the effect of prewetting the paste electrolyte with lithium and selenium on cell performance (2) to test the effect on cell performance of forced contact between the paste electrolyte and the lithium-containing stainless steel felt, and (3) to test a modification in the cathode cup designed to prevent radial expansion of the paste electrolyte.

Several major changes were made in the design and assembly of Cell No. 5:

a. The paste electrolyte was not wetted with selenium prior to cell startup.

b. The cathode housing contained a depressed sealing surface to prevent radial expansion of the paste electrolyte.

c. Cell clamping forces were more effectively applied to

ensure good electrical contact between the lithium-containing stainless steel felt and the paste electrolyte. Normally, the boron nitride ring depressed the paste electrolyte to ensure good sealing of the anode and cathode materials. For Cell No. 5, the boron nitride ring pressed the stainless steel felt, containing lithium, against the paste electrolyte.

Some of the above features are shown in Fig. 1C. (The Inconel springs shown in this figure were not used for Cell No. 5, and a stainless steel O ring was used, as shown in Fig. 1B.)

Figure 4 shows a typical voltage-capacity density curve for Cell No. 5 (taken at constant current). The cell was discharged at 0.31 and 0.49 A/cm^2 (9.7 and 15.6 A) for 15 and 10 min, respectively. No capacity measurements were made for this cell since difficulty was experienced during recharging.

The results of short-time voltage-current density measurements for Cell No. 5 are shown in Fig. 5. The best short-circuit current density, measured during the first day of testing, was 3.8 A/cm^2 (120 A). The resistivity of the paste electrolyte was 2.24 ohm-cm, corresponding to the 3.8-A/cm^2 short-circuit current density. The resistivity ratio was 6; the theoretical resistivity ratio was 1.85. The internal resistance of the cell increased during the testing period, and difficulty was experienced in recharging the cell. The cell voltage dropped, typical of cell shorting. The cell was cooled to room temperature and checked for shorting, An accumulation of Li_2Se (identified by chemical analysis) was found between the boron nitride housing, the stainless steel O ring, and the cathode housing. This material was removed, and the cell was electrically checked again. Cell performance did not improve.

f. Test Results for Cells No. 6 and 7

The objective of these experiments was to determine the reproducibility of cell performance. Cells No. 6 and 7 were assembled identically (similar to the cell shown in Fig. 1C, having an identical cathode cup and spring-loaded paste electrolyte), loaded with different quantities of lithium and selenium, and discharged at 0.15 A/cm^2 (4.8 A) to 1.0 V. The paste electrolytes were not prewetted. Typical voltage-capacity density curves for these two cells are presented in Fig. 3. For both cells, the average voltage during this discharge was 1.6 V. The percent of theoretical capacity achieved for Cell No. 6 was 55.2% and for Cell No. 7, 58.8%. A comparison of cell voltages as a function of percent of capacity discharged indicates that the reproducibility of capacity density at a given current density is adequate for design purposes. A charging curve for Cell No. 7 is shown in Fig. 3. No explanation was apparent for the unusual shape of this curve. The IR-free charging curve is an approximate curve, because voltages were measured at set time intervals, whereas the IR-included curve is plotted from continuous voltage measurements with time.

Short-time voltage-current density measurements for Cell No. 7 are presented in Fig. 5. During constant-current discharge, the resistances of Cells No. 6 and 7 were nearly the same. However, these values were slightly different from the cell resistances determined from short-time voltage-current density measurements prior to constant-current discharge. The cell resistivities were 11.4 and 12.2 ohm-cm for Cells No. 6 and 7, respectively, during short-time voltage-current density measurements. The resistivity of the cells determined from the constant-current measurements was approximately 7.2 ohm-cm. This decrease in cell resistance was probably the result of increased wetting of the paste electrolyte by lithium during discharge. Cells No. 6 and 7 performed well during the first day of testing. After the cells were recharged and stood on open circuit overnight at 400°C, the internal resistance of the cells had increased substantially.

The cells were examined after shutdown. In both cases, the paste electrolyte showed reddish discoloration on the selenium side, typical of diffusion by some cell material. Selenium is not very soluble in the electrolyte (approximately 0.03 mol % at 400°C), but the question is raised as to the solubility of reaction products. Measurements will be made to determine the solubility of Li_2Se in the LiF-LiCl-LiI eutectic, and tests will be made to determine cell modifications needed to eliminate transfer of materials through the paste electrolyte.

g. Test Results for Cell No. 8

The objective of this experiment was to test the cell design shown in Fig. 1C. This design contains modifications intended to eliminate the shortcomings identified in tests of Cells No. 1 to 7, especially with regard to the achievement of high performance and good sealing of selenium in the cathode compartment. The essential features of this cell include (1) spring-loading of the lithium-soaked stainless steel Feltmetal, to provide good contact with the paste electrolyte; (2) a boron nitride ring, to serve as the anode housing (sealing the lithium in the anode compartment) and as an anode insulator (preventing lithium deposition outside the cell during charging); (3) grooving of the cathode-compartment sealing surface, to provide a tight selenium seal on heating the cell (the space for volume changes of the paste electrolyte on heating were restricted, except for the grooves on the sealing surface); and (4) welding the cathode-current collector (niobium expanded mesh) to the cathode cup, to provide good electrical contact.

The cell was operated in the usual manner with the paste electrolyte in the vertical position and with about 50% voids in the cathode compartment to allow for lithium transfer.

Figure 4 shows a typical voltage-capacity density curve for Cell No. 8. This cell was discharged at 400°C to 1.0 V at

a current density of 0.52 A/cm^2 (16.5 A). The average voltage during this discharge was 1.4 V; 38% of theoretical capacity was achieved. The sharp initial drop in the discharge curve is a result of poor wetting of the paste electrolyte by lithium. As wetting occurs, the IR-included cell voltage rises. No explanation was apparent for the large increase in the IR-included charge curve shown in Fig. 4. A concentrated effort will be made in future cell tests to improve the charge characteristics of these cells.

Short-time voltage-current density data for Cell No. 8 are presented in Fig. 5. The peak power density for this cell was about 1 W/cm^2. Resistivities for the paste electrolyte at the beginning of discharge measurements and after charging for several hours were 4.4 and 3.9 ohm-cm, respectively. After an overnight period of charging at 0.0032 A/cm^2 (0.1 A), the open-circuit voltage had dropped from 2.04 to 1.94 V, and the resistivity had increased to 17.1 ohm-cm. The cell was shut down and examined. The increased resistance resulted from formation of Li_2Se at the lithium/paste-electrolyte interface. Future cell tests will be made in an attempt to eliminate the formation of Li_2Se on the lithium side of the paste.

h. Conclusions from the Tests of Cells No. 1-8

Based upon the initial performance tests for 7.5-cm-diam paste-electrolyte cells, the following conclusions can be drawn:

(1) A technique is needed to enhance wetting of the paste electrolyte by lithium. Lack of wetting in some cells has resulted in high internal resistance and correspondingly poor electrical performance. (Wetting techniques are being investigated under Task B, Studies of Paste Electrolytes for Lithium/Selenium Cells.)

(2) The major factors contributing to good cell performance, outlined under Test Results for Cell No. 8, have been defined. Performance measurements have been made for operating times up to 50 hr. The maximum number of cycles for the cells tested was 10 cycles, and the discharge rates ranged from 0.5 to 2 hr. Peak power densitites of 1 to 2 W/cm^2 which can be maintained for several seconds, are also reproducible from cell to cell.

(3) A major effort is required to identify those conditions required to maintain high cell performance over long periods of time and for a large number of charge-discharge cycles. One important aspect is the undesirable transport of selenium to the anode compartment.

B. LIFE TESTING AND CHARGE-DISCHARGE CYCLE TESTING OF LITHIUM/SELENIUM CELLS

(V. M. Kolba and J. D. Arntzen)

This phase of the program is being devoted to lifetime and charge-discharge cycle testing of cells. Concepts developed from the cell-performance studies discussed in Section II.A above will be tested and evaluated during charge-discharge cycles for operating times up to 2000 hr. Various charge-discharge cycles will be investigated to determine cell response to various rates and levels of operation over extended periods of time; cell internal resistance will be measured. Information on the effectiveness of various sealing methods and on the structural stability of the components will be obtained.

Two furnaces and associated equipment are being installed in a vacuum-frame hood. Stainless steel furnace tubes for cell testing in a helium atmosphere of $\leq$5 psig are in place. Power for the cells will be supplied from the regulated power supply serving the existing test facility. Each furnace will have controls with valving to a common vacuum, helium, and vent system. Each test location will have variable-load resistors, a temperature recorder, and a voltage-current recorder. By appropriate switching, one of the voltage-current recorders will be used for short-term data measurements of both test facilities.

Pending design and development of vacuum-tight cells capable of being exposed to the atmosphere, cells will be assembled in an inert-atmosphere box and placed in the furnace tube; the tube will be sealed and then moved from the glovebox to the furnace for testing.

Table III lists tentative values of the variables to be used during the testing. Initially, voltage-current density data and voltage-time data at constant current will be taken approximately twice a day. The internal resistance of the cell will be determined periodically, as required.

The long-range goal of the charge-discharge cycle testing portion of the program is to develop reliable cells for a 50-kW battery to be used in an electric vehicle-drive system. The battery-voltage requirements [3] are 160 V open circuit and 100 V minimum. A reasonable test-power profile [3] consists of a discharge sequence of 50 kW for the first 3 sec, 25 kW for the next 40 sec, and 3.7 kW for the final 57 sec, followed by charging at 50 kW for 3 sec, 25 kW for 7 sec, and some lower power level (of not less than the 1-hr rate) for the time necessary to replace the energy removed during the discharge cycle. This cycle is to be repeated for 100 cycles without any special catch-up

TABLE III. Values for Variables To Be Used in Cell Life Tests

	Goals
Temperature	400°C and lower
Atmosphere	Helium
Pressure (external to cell)	$\leq$5 psig
Total time	$\geq$2000 hr
Voltage	
Charge	2.2 V max, open circuit
Discharge	1.0 V min
Current density (constant current)	
Discharge to 1 V	1-hr rate
Discharge to 1 V	0.5 A/cm^2
Charge to 2.2 V	Max feasible current
Charge to 2.2 V	1-hr rate

period. The number of lithium/selenium cells required to meet these voltage and power requirements is estimated as follows:

$$\text{Number of series-connected cells} = \frac{160\ \text{V}}{2.20\ \text{V/cell}} \cong 73.$$

For a battery of 73 large-area cells (connected in series), each cell would be required to deliver 685 W for 3 sec, 342 W for 40 sec, and 51 W for 57 sec; this would require 22.6-cm-diam cells. If the battery were to be constructed from a number of 73-cell stacks of 7.5-cm-diam cells connected in parallel, 12 such stacks would be required (corresponding to about 2 W/cm^2 at the 50-kW total power point). The most reasonable compromise between one stack of relatively large-diameter cells and 12 stacks of 7.5-cm-diam cells might be two stacks of 16-cm-diam cells. Future investigations should therefore include scale-up to cells of about 16-cm diameter, as a step in seeking the best cell size for use in the 50-kW battery.

C. DESIGN OF HIGH-SPECIFIC-POWER LITHIUM/SELENIUM CELLS (V. M. Kolba)

This phase of the program is devoted to the development of cell designs that will reduce the weight of each cell and yet provide performance as high as, or higher than, that demonstrated in the cell-performance studies described in Section II.A. Because of the limited cell-design experience using lightweight structural materials, no attempt was made to design a minimum-weight unit, but rather to design a lighter-weight cell believed to have a reasonable chance of achieving the electrical performance of the cells presently being tested. Sufficient design and test data will be generated to permit reliable projections of designs to minimum-weight systems.

Prototype designs will be tested as described in Section II.B. Upon successful completion of these tests, a sufficient number of cells of the chosen design will be fabricated and tested to permit a statistical evaluation of the variables in electrical-performance measurements during life testing.

Some preliminary designs have evolved and are being evaluated in terms of the problem areas of sealing, differential thermal expansion, dimensional tolerances, insulation, and methods of component fabrication within the confines of the presently available paste-electrolyte technology and available fabricating facilities.

Figure 9 is a preliminary sketch of a design for a lightweight cell, modified for testing purposes. A V-ring clamp, which wedges on the insulated periphery of the end cups, is used to hold together the flanges, boron nitride insulators, and a V ring, which seals against the paste electrolyte. To ensure contact at the paste-electrolyte interface, pressure is applied to the lithium-stainless steel felt and selenium-niobium mesh sections by wave springs at the bottom of each electrode compartment. This design should permit the paste electrolyte to accommodate expansion differences while maintaining a selenium-tight seal.

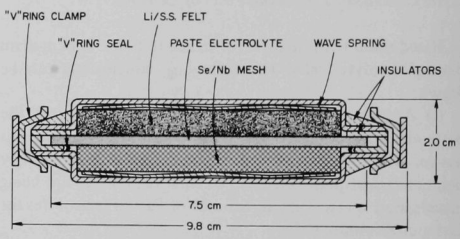

Fig. 9. Proposed 7.5-cm-diam Paste-electrolyte Test Cell.

III. PASTE-ELECTROLYTE STUDIES

A. PHYSICOCHEMICAL PROPERTIES OF PASTE ELECTROLYTES (L. E. Trevorrow and J. G. Riha)

The objective of this work described is to develop paste electrolytes with physicochemical properties that will approach an optimum combination of conductivity, strength, and wettability by molten lithium. (Paste-electrolyte wetting by selenium does not appear to be a problem.) The experimental work therefore includes fabrication of paste disks, using a selection of materials and procedures; and testing the disks to measure their electrical resistance, mechanical or rheological properties, and wettability. The results of this investigation will be particularly useful in fabricating large-diameter electrolyte disks (greater than 7.5-cm diameter) of good strength and low electrolytic resistance. Also, the electrolytic-resistance measurements are required to determine the lower resistance limit achievable in paste-electrolyte cells in order to optimize performance. This report describes initial experiments involving fabrication of paste-electrolyte disks and presents some observations of their electrical resistances and wettability by molten lithium.

1. Fabrication of Paste-electrolyte Disks

Paste-electrolyte disks were fabricated from 11.7 mol % LiF-29.1 mol % LiCl-59.2 mol % LiI eutectic mixture and lithium aluminate filler prepared by the Institute of Gas Technology from γ-alumina obtained from two commercial sources (Degussa, Inc., Kearny, New Jersey; and Linde Company, Division of Union Carbide Corporation,

New York, N.Y.). A typical procedure for mixing a batch of salt and filler before pressing into disks involved heating the mixture (in a helium atmosphere) in beakers of either quartz or alumina at 500°C for three 3-hr periods. The use of quartz was discontinued in the early stages of this work, however, since a slight attack of quartz by the mixture was observed. The mixture was ground with a porcelain mortar and pestle before and after each heating period. During heating, mixtures containing the Degussa material agglomerated into gray cakes that were easily broken; mixtures containing the Linde material remained in the form of a loose powder with little color change. Disks were pressed in vacuo at room temperature with a pressure of 1050 kg/cm^2. The nominal composition of each disk was 60 wt % salt-40 wt % filler. The diameter of each disk was 13 mm, and the thicknesses of the disks ranged between 2 and 3 mm. These disks normally had smooth faces and sharp edges.

2. *Electrical Circuit Used in Measuring Resistances of Paste Electrolyte Disks*

The electrical circuit used to test the resistance of paste disks by a dc method is shown schematically in Fig. 10. All components except the sample cell were outside the inert-atmosphere glovebox, the wall of which is shown by the broken line. The resistance of a sample was determined by measuring the current through, and the voltage across, the sample. Switch SW2, when thrown to the left, allowed the voltage across the sample to be measured with the potentiometer (a Leeds and Northrup Model K-3). When Switch SW2 was thrown to the right, the voltage across the standard resistor (R2, 100.00 ohms) was measured. The current through the circuit, and therefore through the paste, was calculated from the voltage drop across this standard resistor using Ohm's law. Switch SW3 permitted a bypass of the resistance R2 if electrochemical deposition of lithium electrodes in situ was desired. The direction of current flow was reversed by Switch SW1. Variable resistance R1 was a decade resistance box that allowed the current in the circuit to be adjusted. The power supply was a lead-acid battery.

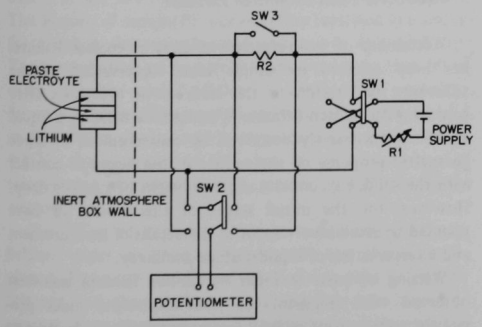

Fig. 10. Circuit Diagram of Apparatus for Electrolyte Resistance Measurements by a DC Method.

3. *Results of Measurement of Electrical Resistances of Paste-electrolyte Disks*

Table IV lists the resistivities obtained for three paste-electrolyte disks. In each test, the resistivity decreased from a much higher initial value to a steady value, probably indicating the establishment of steady-state interfacial conditions. The steady values are listed in Table IV. The resistance measurements of samples P1 and P2 were made with a sample holder similar to that shown in Fig. 11. For these measurements, however, a paste-electrolyte disk was pressed between two stainless steel tubes filled with molten lithium, instead of the Feltmetal disks shown in Fig. 11. Electrical measurements could not be obtained for two samples fabricated from lithium aluminate prepared from Degussa γ-alumina, because in both instances the edges of the opposing tubes of the conductivity apparatus cut through the disk, resulting in a short circuit. This observation suggests that the strength of disks made from Degussa material may be inferior to that of disks made from Linde material, possibly because the Degussa material had a lower specific surface area (15 m^2/g) than the Linde material (46 m^2/g).

For sample P1, current was continuously passed through the disk for about 5 hr and resistivity measurements were made at various intervals. For sample P2, although the disk was held at 400°C for about 4 hr, current was passed through it only during resistance measurements. Because of the passage of greater current through sample P1, deposition of lithium at the paste surface may have improved the contact between the disk surface and molten lithium,

TABLE IV. Properties of Paste-electrolyte Disks

Salt:	LiF-LiCl-LiI eutectic
Filler:	Lithium aluminate prepared by Institute of Gas Technology from γ-alumina (Linde)
Nominal composition:	60 wt % salt, 40 wt % filler
Disk diameter:	13 mm
Pressing conditions:	1050 kg/cm^2 in vacuo at room temperature

Sample No.	Observed Density at 25°C, g/cm^3	Temperature at Resistance Measurement, °C	Resistivity, ohm-cm	Approximate Resistivity Ratio
P1	3.0	400	3.2	7
P2	2.8	400	10.2	21
P16	2.8	360	1.5	3

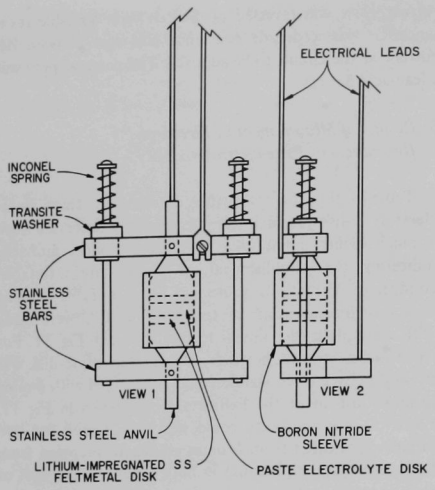

Fig. 11. Sample-holder Assembly No. 2 for Resistance Measurements in Paste-electrolyte Disks.

resulting in the lower apparent resistivity. On the other hand, the resistivity value obtained for P1 may have been low because of error in the electrode area used to calculate the resistivity; some lithium had crept out around the edges of the containing tube, possibly increasing the area of electrical contact between the lithium and the disk surface. Examination of the paste electrolyte disks after removal from the sample holder showed that lithium adhered to only small fractions of the total cross-sectional area exposed to molten lithium.

The electrical conductivity of paste-electrolyte disk P16 was measured with the sample holder shown in Fig. 11. In this sample holder, a paste-electrolyte disk was pressed between two stainless steel felt disks (Huyck Type 302, 1.6-mm thickness, 90% porosity, 67-μ mean pore diameter) soaked with lithium. The diameters of the lithium-soaked disks were the same as that of the paste-electrolyte disk. The peripheral surface of the disk sandwich was supported by an insulating cylindrical sleeve of boron nitride.

Before this conductivity experiment, paste-electrolyte disk P16 had received the following special conditioning treatment: The disk was supported on a stainless steel stirrup just above a crucible of lithium at 520°C for about 16 hr in a helium atmosphere. This conditioning treatment, to promote the subsequent wettability of the paste-electrolyte disk, was chosen on the basis of wetting observations described below.

The results of the resistivity measurements of paste-electrolyte disk P16 are recorded in Table IV. In previous discussions of the resistivity of paste electrolytes [1], the ratio of the resistivity of the paste-electrolyte to the resistivity of the pure electrolyte, K_m^{-1}, has been compared with the ratio calculated from the Maxwell relation, $K_m^{-1} = (2 + f)/(2 - 2f)$, where f is the volume fraction of filler. The ratio calculated from the Maxwell relation possibly represents the lower limit that can be realized for paste electrolytes. The resistivity ratio of paste-electrolyte disk P16 was about 3 (subject to minor corrections for thermal expansion of the paste), roughly 1-1/2 times as great as the ratio calculated from the Maxwell relation.

After this measurement, an examination of the sample-holder assembly disclosed evidence of chemical attack on the boron nitride sleeve with the formation of a black ring in the neighborhood of the paste-disk sandwich. The sample of boron nitride used in this experiment is considered to be inferior with respect to oxygen impurity. Since the black material had a low electrical resistance, the validity of the conductivity measurement is questionable. Examination of the sample at room temperature showed that although the lithium-soaked stainless steel felt disks adhered strongly to the paste-electrolyte disk, contact at the edges of the disks was not good. When the lithium-impregnated disks were cut away, about 30% of the area of one face and about 50% of the area of the opposite face were covered with adherent lithium. The fraction of total interfacial area wetted would probably have been increased if the pressure on the sandwich had been great enough to provide good contact between the stainless steel disks and the paste-electrolyte disk at the edges.

Present efforts in the area of measurements of resistance of paste electrolytes are aimed at the development of a sample-holder assembly that will provide for accurate measurements. Some of the problems indicated in the preceding paragraph can be eliminated, since recent trials have shown that a sleeve is unnecessary.

4. Observations of the Wettability of Paste-electrolyte Disks by Molten Lithium

Wettability of paste-electrolyte disks by molten lithium has been assessed by simple visual observation of the adherence of lithium to the surfaces of the disks after contact with molten lithium. Wetting of a solid by a liquid can be quantitatively described by measurement of some geometric property of the surface of the liquid in contact with the solid, e.g., contact angle or height of a sessile drop. However, for the initial stages of this work, we have planned to avoid involvement in the details of measurement and interpretation of liquid surface geometry.

Wetting of paste surfaces by molten lithium was first observed with fragments of paste-electrolyte disks previously used in conductivity experiments. Those fragments were used that had areas previously unexposed to molten lithium. Each fragment was floated on a molten-lithium

pool and was removed occasionally to observe the underside. Paste fragments placed on molten lithium at 400°C slid on the surface of the liquid in a manner similar to grease sliding on water. The fragments darkened in color and showed tiny areas of adhering lithium. Fragments floating on molten lithium at 450-500°C darkened more rapidly, becoming black, but they showed areas of adhering lithium that increased in size as the time of exposure to lithium increased. Surfaces of paste fragments lost their smooth appearance at 450°C and showed pitting at 500°C, possibly the result of dissolution of electrolyte in molten lithium. One paste fragment was completely covered with an adherent coating of lithium after floating on liquid lithium for 30 min at 450°C, cooling to room temperature overnight, and then floating on liquid lithium for an additional 2 hr at 450°C.

On the assumption that pitting of paste surfaces in contact with molten lithium was the result of dissolution of eutectic salt in the lithium, saturation of lithium with eutectic would probably eliminate this pitting problem. Additional wetting experiments were carried out using a molten-lithium pool previously saturated with salt. The surface of a pool of molten lithium, contained in a stainless steel cup, was skimmed with a loop of stainless steel wire to remove the surface scum; then a small amount of LiF-LiCl-LiI eutectic was stirred into the lithium. Upon melting, the eutectic salt acted as a flux, causing the lithium to wet the stainless steel cup rapidly. After the molten-lithium surface had been skimmed again, disk P1, intact after previous use in electrical conductivity experiments, was floated on the molten-lithium surface at about 350°C. Lithium had not adhered to this disk during conductivity experiments in which it was in contact with molten lithium for several hours; but after 45 min of floating on the molten-lithium pool, the entire side in contact with the lithium pool (except for two small circular areas) was covered with a bright, adherent coating of lithium. However, duplication of this procedure with a freshly pressed disk, P5, did not result in an adherent coating of lithium. The history of sample P1 was therefore reviewed in a search for variables that may have contributed to its wettability. The composition of sample P1 was similar to that of all other samples tested (60 wt % LiF-LiCl-LiI eutectic-40 wt % lithium aluminate). Since sample P1 had been held in the electrical-conductivity apparatus for about 6 hr at 400°C, the exposure of the paste to lithium at elevated temperature was suspected of promoting the subsequent wetting.

The effect of exposing other paste-electrolyte disks to lithium vapor at elevated temperature was therefore explored. Exposure to lithium vapor rather than to molten lithium was chosen since vapor exposure was easier to control experimentally than exposure to salt-saturated molten lithium. Whole paste-electrolyte disks, rather than fragments, were subjected to a conditioning procedure consisting of suspending the disks in the furnace well on a stainless steel stirrup located directly over a crucible of lithium. Three paste-electrolyte disks were treated in this manner at 530°C for about 16 hr. Each disk was then cooled very slowly to about 200°C to avoid cracking. Although the disks were blackened by this treatment, they retained their shapes and sharp edges. Each disk was then placed on the surface of a pool of molten lithium at 350-360°C that had been treated with a small amount of LiF-LiCl-LiI eutectic. After the disk had floated on the pool for 30 min, the system was cooled slightly to allow the salt in the disk to freeze, thereby avoiding distortion of the disk when recovering it from the pool. The paste-electrolyte disks were then lifted from the surface with forceps and examined. In each of the three cases, the entire underside of the disk was coated with lithium, indicating that the process was effective in promoting the wettability of the disks. Theories of the wetting process commonly assume adsorptive covering of the solid surface by molecules of the wetting fluid. Exposure of the paste electrolyte to lithium vapor may be a suitable condition for the occurrence of the absorptive mechanism.

Some material (presumably lithium halide) had sublimed from each paste-electrolyte disk and condensed on the cooler portions of the furnace well during the vapor-conditioning treatment at 530°C described above. To avoid this undesirable sublimation, a conditioning treatment using a lower temperature was tried. An additional paste-electrolyte disk was treated by a procedure similar to that described above, except that the temperature was maintained at 444°C. In the subsequent wetting test at 350°C, lithium did not readily adhere to this paste-electrolyte disk. A conditioning treatment similar to that described above, but using some temperature between 444 and 530°C, might provide the desired wettability without altering the eutectic composition by sublimation of alkali halides.

The possibility of using a vacuum-evaporation procedure to coat paste-electrolyte disks with lithium is also being explored. This arrangement would permit an initial vacuum bake-out of a paste-electrolyte-disk surface followed by heating a lithium source in the presence of the exposed paste surface. The temperatures of the lithium source and the paste-electrolyte disk might then be controlled separately to arrive at a suitable coating procedure.

B. FABRICATION OF 7.5-cm-diam PASTE-ELECTROLYTE DISKS (E.C. Gay and J. E. Kincinas)

Paste-electrolyte disks of 7.5-cm-diameter have been prepared to determine the effect of temperature and specific surface area of ceramic filler on paste density. The objective of this investigation is to determine the optimum pressing conditions required to prepare paste-electrolyte disks of high strength and low resistivity.

Table V shows densities of 7.5-cm-diam paste-electrolyte disks prepared under various conditions. Parameters varied in these electrolyte preparations included sources of Al_2O_3 for reaction with Li_2CO_3 to prepare the filler, reaction conditions, pressing temperature, and pressing time. These paste-electrolyte disks were prepared with LiF-LiCl-LiI eutectic and lithium aluminate filler. The salts used to prepare the LiF-LiCl-LiI eutectic were reagent-grade materials (purities of 99.3% LiCl, 71-73% LiI, and >99.9% LiF), further purified by lithium contact to remove water and heavy metals. The filler density was measured with an air-comparison pycnometer, and the chemical composition (i.e., γ-Al_2O_3, one of the starting materials; and α-$LiAlO_2$ and/or γ-$LiAlO_2$, the expected major products at 500 and 800°C, respectively) was determined from X-ray diffraction analyses. The specific surface area of the filler was measured with an automatic BET surface-area analyzer.

As shown in Table V, paste electrolytes were prepared with densitites from 70 to 99% of the theoretical values. Although the optimum pressing conditions have not yet been determined, these data show that high-density paste electrolytes can be prepared from both α-$LiAlO_2$ and γ-$LiAlO_2$. Hot pressing under vacuum appears to be necessary for high density in the present pressing apparatus.

An advantage of the mold currently being used is that vacuum can be applied to the paste-electrolyte mixture at elevated temperatures while maintaining a uniform disk thickness. Disks have been prepared with only 0.076-mm (3-mil) thickness difference across the face of the disk. (Typical electrolyte thicknesses ranged between 2 and 3 mm.) Different leveling techniques are being tested to determine the best method of ensuring the thickness uniformity.

A minor disadvantage of the present pressing apparatus is the difficulty of ejecting the paste-electrolyte disk after pressing. The high temperature required for high density enhances reaction between the eutectic salt and the mold material. The result is bonding between the paste-electrolyte cylindrical edges and the mold. Cracking of the disks frequently resulted when the paste electrolyte was ejected. Before disk No. 13 was prepared, the cylindrical walls of the mold were coated with a molybdenum disulfide solution. This material is stable under vacuum up to 650°C. High-density paste electrolytes are now ejected from the mold without cracking or chipping the edges, and the MoS_2 coating has not caused contamination of the paste-electrolyte surface. The capability now exists for routine fabrication of 7.5-cm-diam paste electrolyte with densities up to 95% of the theoretical values.

TABLE V. Densities of 7.5-cm-diam Paste Electrolyte Prepared under Various Conditions at 56,600-kg Force Using LiF-LiCl-LiI Eutectic Electrolyte

Disk No.	Filler Surface Area,[a] m^2/g	Filler Density,[b] g/cm^3	Pressing[c] Temp, °C	Pressing Time, min	Paste-electrolyte Density, g/cm^3	Fraction of Theoretical Density[d]	Used in Cell No.[e]
1	34.8	3.83	~250	15	3.26	0.89	1
2	35.8	3.88	25	15	2.80	0.77	2
3	35.8	3.88	25	15	2.75	0.76	-
3A	35.8	3.88	25	15	2.95	0.81	-
4	46.3	3.28	165	15	2.39	0.70[f]	3
5	-	2.89	260	15	3.27	0.99	-
6	-	2.89	275	15	2.97	0.90	-
7	-	2.89	270	15	3.26	0.99	-
8	-	2.89	25	60	2.55	0.77	4
9	46.3	3.28	170	15	2.86	0.84	-
10	46.3	3.28	209	15	3.17	0.93	-
11	46.3	3.28	188	60	3.17	0.93	-
12	46.3	3.28	188	60	3.14	0.92	-
13	46.3	3.28	153	60	2.90	0.85	5
14	-	3.22	174	15	3.13	0.92	6
15	46.3	3.28	172	15	2.82	0.83	7
16	46.3	3.28	196	15	3.10	0.91	8
17	46.3	3.28	252	15	3.21	0.94	-
18	46.3	3.28	253	15	3.27	0.96	-
19	46.3	3.28	201	60	3.26	0.96	-
20	46.3	3.28	195	60	3.22	0.94	-

[a]The lithium aluminate filler used in paste electrolytes 1-4 and 9-20 was predominantly α-$LiAlO_2$. The filler for paste electrolytes 5-8 was predominantly γ-$LiAlO_2$. Differences in filler surface area result from use of different commercial sources of Al_2O_3 (different surface area and particle size) in preparation of the filler.

[b]The differences in the filler pycnometer densities are a result of the varying quantities of α-$LiAlO_2$ and γ-$LiAlO_2$ in the mixtures.

[c]All the paste electrolytes were pressed under vacuum.

[d]Theoretical densities were calculated using LiF-LiCl-LiI pycnometer density = 3.50 g/cm^3.

[e]The paste composition was the same (60 wt % electrolyte) for the paste disks used in these cells in order to compare electrical performances and make design changes to improve performance.

[f]In general, the low-density paste electrolyte had insufficient strength for use with normal cell clamping forces without cracking. These electrolytes were tested, however, to determine the lowest electrolyte density of adequate strength for use in the cells.

IV. SEALANTS AND INSULATORS
(M. L. Kyle, P. W. Krause, and F. J. Martino)

Lithium/selenium cells require electrically insulating materials resistant to lithium, selenium, and lithium-selenium alloys. These cells may also require a sealant resistant to attack in order to produce a hermetically sealed battery.

Boron nitride is currently being used as the electrically insulating material in test cells. This material has performed well in service, but inspection of cells after operation has indicated that boron nitride is not completely immune to attack by lithium-selenium mixtures [corrosion rate estimated to be 0.5 mm/yr (20 mils/yr)]. Consequently, other insulating materials are being evaluated in this program, but this is not a major effort, since boron nitride appears adequate for the cells that will be operated for about 1000 hr. In addition, boron nitride is readily machinable and can easily be fabricated for test-cell parts.

Two other electrically insulating materials have been evaluated recently. Single-crystal magnesia (MgO) and yttria (Y_2O_3) showed corrosion rates of 0.65 and 1.8 mm/yr (26 and 71 mils/yr), respectively, after immersion in a selenium-20 at. % lithium mixture at 375°C for about 300 hr. Neither material appears to be as corrosion-resistant as boron nitride. Other materials, such as thoria (ThO_2) and aluminum nitride (AlN), which have demonstrated good resistance to molten lithium at 375°C [4], will be tested for resistance to lithium-selenium mixtures.

Several high-temperature polymers were tested for thermal stability in helium and resistance to lithium and lithium-selenium mixtures. Insulating polymers are being investigated because they potentially offer both electrical insulating and hermetic sealing capabilities in a thin lightweight form, which could reduce both the size and weight of a battery. Screening tests to determine thermal stability (in helium) of silicone resins, polyimides, and a polycarboranesiloxane resin were performed in a cup-like apparatus. In these tests, the sealant was placed in a groove cut into a Type 304 stainless steel plate, and a stainless steel tube was placed into the groove so that the cured sealant provided a bond between the tube and the plate. The sealant was cured according to the manufacturer's suggested procedure, and the cured sealant specimens were maintained at 375°C in a helium atmosphere. The results of these tests are presented in Table VI. These tests demonstrated that some of the polymers, especially the polyimides and polycarboranesiloxane resin, possess reasonable thermal stability in helium so that they may be useful in some applications which require electrical insulation.

The corrosion resistance of these same polymers was determined in various systems of interest, as shown in Table VII. The polyimide and polycarboranesiloxane resins were tested more extensively because their apparently greater thermal stability made them potentially better candidates for cell application. These tests showed that although the polymers appear to posses adequate thermal stability and are corrosion-resistant to liquid lithium at 190°C for short times, the polymers were destroyed when exposed to simulated cell conditions. An alternate method of using these polymers as corrosion-resistant insulating materials is being evaluated [4]. In this method, about one-third polymer (by weight) is mixed with two-thirds lithium aluminate, and the composite material is used as the insulator. In all cases of >5 mm/yr (200 mils/yr), preliminary tests of Pyre ML and lithium aluminate (the Pyre ML is actually a binder to enable molding and forming of desired shapes from lithium aluminate) exposed at 375°C to lithium (260-hr exposure), selenium (233-hr exposure),

TABLE VI. Thermal Stability of Polymeric Materials in a Helium Atmosphere

Temperature: 375°C; pressure: 1 atm

Polymer	Type	Test Duration, hr	Results
Pyre ML[a]	Polyimide	137	Sample intact; insulating.
Pyre ML[a]	Polyimide	311	Discolored; resistance >20 megohms.
Dexsil 202[b]	Polycarboranesiloxane	311	Discolored; resistance >20 megohms.
DC-R-7521[c]	Silicone Resin	137	Sample badly cracked.
XR-6-3502[c]	Silicone Resin	137	Sample intact; insulating.
GE-SR-82[d]	Silicone Resin	137	Sample badly cracked.
CHR-TEMP-R-TAPE[e]	Polyimide Film, Silicone Resin Adhesive	137	Polyimide tape intact.

[a]Product of E. I. duPont de Nemours and Company, Inc.
[b]Product of Olin Mathieson Corporation.
[c]Product of Dow Corning Corporation.
[d]Product of General Electric Corporation.
[e]Product of Connecticut Hard Rubber Company.

TABLE VII. Corrosion Resistance of Polymeric Materials to the Lithium/Selenium System

Polymer	System	Test Duration, hr	Temp, °C	Results
Pyre ML	Lithium	119	190	Intact.
Pyre ML	Se-20 at. % Li	311	375	Polymer destroyed.
Dexsil 202	Se-20 at. % Li	311	375	Polymer destroyed.
DC-R-7521	Lithium	119	190	Discolored and cracked.
XR-6-3502	Lithium	119	190	Intact.
GE-SR-82	Lithium	119	190	Polymer destroyed.
CHR-TEMP-R-TAPE	Lithium	119	190	Tape intact; adhesive failed.

and selenium-20 at. % lithium (233-hr exposure) have been unsuccessful with observed corrosion rates. The use of these polymers may be limited to applications in which thermal stability is required in the absence of lithium or selenium. Such an application would be insulation of electrical leads or insulation of the external cell parts.

V. CORROSION BY LITHIUM-SELENIUM MIXTURES

(M. L. Kyle, P. W. Krause, and F. J. Martino)

The development of reliable, long-lived lithium/selenium secondary batteries requires corrosion-resistant materials. Since selenium, lithium, and the molten salts used in these cells are relatively reactive, they are corrosive to many common materials. The selection of suitable corrosion-resistant materials is a major requirement for the successful utilization of these batteries.

A variety of materials will be needed to meet the varied cell requirements. Table VIII indicates the material requirements for a typical lithium/selenium battery. Corrosion resistance is the most important quality of a desirable construction material, but is not the sole criterion for materials selection. Some of the other factors that are important in selecting the proper materials include density, since a lighter-weight construction material would increase the specific energy of the battery, and ease of fabrication, since some parts of the cell such as the current collectors require a fabricated structure difficult to produce with some materials.

The corrosion of metallic conductors by molten lithium is not being extensively investigated at present, because the containment of lithium and current collection from it can probably be done with austenitic stainless steels or similar conventional materials. These steels have performed well in laboratory tests for several hundred hours.

TABLE VIII. Outline of Battery Materials Requirements

Cell Component	Materials Requirement[a]
Anode compartment	Electronic conductor resistant to molten lithium; any corrosion product must be conductive.
Cathode compartment	Electronic conductor resistant to molten selenium and lithium-selenium alloys; any corrosion product must be conductive.
Electrical insulators	Resistant to lithium, selenium, and molten salt; high density to preclude absorption of reactants.
Case, clamps, sealants, insulation	Requirements vary, but materials will be needed to properly encase the battery, maintain its operating temperature, and exclude air during operation.

[a]In addition to the requirements listed, all components must possess acceptable physical properties such as tensile, shear, and creep strength, ductility, and elasticity.

Current program emphasis is on the cathode compartment, which requires a material resistant to the selenium and lithium-selenium alloys that are present in the cathode compartment in the partially discharged state. A 20 at. % lithium-selenium mixture was chosen as representative of the cell in the partially discharged condition. A lithium-selenium alloy is used rather than pure selenium because of the observation that synergistic corrosive effects may occur. The presence of lithium (a strong reducing agent) may preclude containment of lithium-selenium alloys in any metal whose primary corrosion resistance is obtained as the result of an oxide surface film (Li_2O is more stable than Li_2Se). Consequently, corrosion testing of potential cell-containment materials should approximate cell operating conditions.

The corrosion resistance of a variety of potential cathode-housing and current-collector materials to 20 at. % Li-Se mixtures at 375°C was measured in isothermal capsule tests for about 300 hr. The results of these tests are listed in Table IX. The alloy compositions are given in Table X. Figure 12 graphically displays the results of both the metallic-conductor and electrical-insulator tests. These tests were performed by sealing a coupon (~0.3 × 0.3 × 1.5 cm, cut from sheet material) in an evacuated quartz capsule (~2-cm diameter × 6 cm long) containing about 35 g of a 20 at. % Li-Se mixture. The capsules were then held at the test temperature for the desired time. At the conclusion of the tests, the capsules were fractured and the samples were removed. Adhering material was removed by immersion in water at room temperature. (Although selenium is not soluble in water, lithium-selenium mixtures disperse readily in room-temperature water.) The samples were weighed and the weight change was converted to an annual rate for

TABLE IX. Corrosion by 20 at. % Lithium-Selenium Mixtures
Temperature: 375°C

Isothermal Capsule Tests

Material	Exposure Period, hr	Corrosion Rate, mm/yr	Remarks
Niobium	306	0.08	Slight dissolution; possible compound formation
Nb-1% Zr	306	0.11	Nonconductive film formation.
Chromium	328	0.18	
Unitemp 605	233	0.55	
Haynes 25	310.5	0.57	
Cobalt	304	1.3	
Uniloy	306	2.0	
440 SS	309	6.7	
Hastelloy C	304	9.7	
Titanium (75A)	309	14	
405 SS	309	16	
Molybdenum	306	>8.2	Sample destroyed.
Zircaloy-2	311	>45	Sample destroyed.

uniformity of presentation. Some samples were coated with thin films (probably selenides), which were tested for electrical conductivity. The specimens were examined metallographically to determine if any adverse effects, not indicated by the weight-change measurements, had occurred in the specimens. No evidence of intergranular attack at any significant distance from the surface was observed in any sample. In general, attack was almost exclusively due to reaction between selenium and one or more components of the alloy, and the product film thus formed was usually poorly protective. For niobium and niobium-1% zirconium alloy, however, this film (of poor electrical conductivity) was tenaciously adherent.

The results of these tests show that niobium and the niobium-1% zirconium alloys are the most corrosion-resistant materials tested. Chromium and two cobalt-base alloys (Haynes 25 and Unitemp 605) are also corrosion-resistant, and their corrosion rates should be better established in longer-term tests. Other data [4] indicate that beryllium and tungsten may also be corrosion-resistant. The other materials tested are not sufficiently corrosion-resistant for use under cell conditions.

Although the data obtained in these tests are useful for identifying those materials with sufficiently low corrosion rates to be of interest as cell construction materials, they should not be viewed as corrosion rates in operational cells. The data are presented in terms of mm/yr corrosion rates, calculated as the average rate observed in short-term tests of 300-hr duration. Longer-term tests will probably indicate

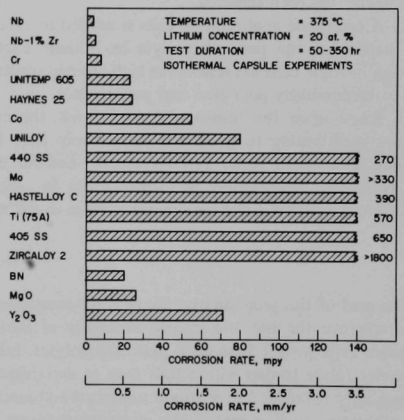

Fig. 12. Corrosion by Lithium-Selenium Mixtures.

TABLE X. Approximate Composition of Alloys Tested in Lithium-Selenium Mixtures

Material	Composition, wt %							
	Fe	Ni	Cr	Ti	Co	W	Mn	Other
Haynes 25[a]	3	10	20	-	Bal[b]	15	1.5	
Unitemp 605[c]	2.6	10	19.6	-	Bal[b]	14.5	1.5	
Uniloy[c]	-	Bal[b]	50	1.0	-	-	-	
440 SS	Bal[b]	-	17	-	-	-	1	
Hastelloy C[a]	6	Bal[b]	15.5	-	2.5	4	-	16 Mo
405 SS	Bal[b]	-	13	-	-	-	1	0.2 Al
Zircaloy-2	0.12	0.005	0.10	-	-	-	-	1.5 Sn, Bal[b] Zr

[a]Product of Union Carbide Corporation.
[b]Balance of composition.
[c]Product of Cyclops Corporation.

lower annual corrosion rates, since most mechanisms for corrosion have a high initial rate, which steadily decreases with time. Conversely, these rates were obtained in the absence of electrochemical effects which would be present in an operational cell. These effects could significantly alter the observed corrosion rates if they enhance mass transport or affect the nature of the protective surface films produced. Therefore, the data obtained in this part of the program will be used only as a guide. The actual performance of various materials will be determined by the results of long-term cell tests.

VI. CONCLUSIONS

Eight lithium/selenium cells with 7.5-cm-diam paste-electrolyte disks (44.2-cm^2 total area, 31.6-cm^2 active area) have been designed, fabricated, and tested. Short-time peak-power densities up to 2 W/cm^2 were delivered by these cells, and up to 60% of the theoretical capacity density was achieved, based upon Li_2Se as the cathode composition at full discharge, at a current density of 0.15 A/cm^2. From the initial performance tests for 7.5-cm-diam paste-electrolyte cells, the following conclusions can be drawn:

1. The scale-up of 3.8-cm^2 paste-electrolyte cells to 31.6-cm^2 cells capable of a short-time peak-power density of 2 W/cm^2 has been achieved.

2. A technique applicable to cells is needed to enhance the wetting of the paste electrolyte by lithium. Lack of wetting in some cells has resulted in high internal resistance and correspondingly poor electrical performance.

3. Based upon the results of Cells No. 6-8, the major factors contributing to good cell performance have been defined (mentioned under Test Results for Cell No. 8) to the point that reproducible performance can be achieved for up to 50 hr (10 cycles maximum) at rates in the range 0.5 to 2 hr (1-V cutoff).

4. A major effort in the experimental program is needed to identify those conditions required to maintain high electrical performance over long periods of time and for a large number of charge-discharge cycles.

5. Additional effort is required to prevent the transport of selenium to the lithium electrode compartment.

Initial measurements of paste-electrolyte resistivities indicate that resistivity ratios as low as 3 may be achievable. Wetting experiments have shown that vapor deposition of lithium on the paste enhances the rate of wetting by liquid lithium.

The results of materials stability and corrosion tests have shown that a few high-temperature polymers are stable at 375°C, but are not resistant to lithium at that temperature. Several ceramic materials have been found to be resistant to lithium at 375°C. These materials could serve either as fillers or as electrical insulators. The metals most resistant to lithium-selenium mixtures at 375°C are beryllium [6], niobium, Nb-1% Zr, and chromium. All other metals tested corrode at a rate above 0.50 mm/yr (20 mils/yr).

VII. FUTURE WORK

The goal of this program over the next six-month period is to improve the life and cycling capability of lithium/selenium cells with 7.5-cm-diam paste electrolytes. Future paste-electrolyte studies will include tests to determine gas permeability (as related to selenium transport) and mechanical properties, such as magnitudes of clamping forces that can be applied for sealing purposes at room temperature and at cell operating temperatures. Also, paste-electrolyte properties will be determined for various fillers and electrolytes other than the lithium aluminate and LiF-LiCl-LiI eutectic presently used. These studies will provide information needed to fabricate large-diameter paste-electrolyte disks of optimum strength and electrical conductivity.

In future cell designs, attempts will be made to minimize the cell weight by the use of low-weight housing and current-collector materials. Beryllium is presently the lowest-weight material tested that has demonstrated reasonable corrosion resistance to lithium-selenium mixtures. Since beryllium cathode-current collectors of the desired form, such as Feltmetal or expanded mesh, are not readily available, corrosion tests will be made to identify other lightweight materials that may be used in the cells. Future investigations will also include performance tests on lightweight cells with paste electrolytes of 7.5-cm-diameter.

REFERENCES

1. H. Shimotake, A. K. Fischer, and E. J. Cairns, "Secondary Cells with Lithium Anodes and Paste Electrolytes," in *Proc. of the Fourth Intersociety Energy Conversion Engineering Conference*, September 22-26, Washington, D.C., 1969, p. 538.
2. C. E. Johnson, "Solid-Liquid Phase-Equilibria and Specific Conductivity for the Ternary LiF-LiCl-LiI System," presented at the Amer. Chem. Soc. Meeting, San Francisco, April 1968, Abstr. No. M-128.
3. Dr. J. R. Huff, U.S. Army Mobility Equipment Research and Development Center, Fort Belvoir, Virginia, private communication.
4. *Section V, Chemical Engineering Division Annual Report–1969*, ANL-7675 (Apr 1970).